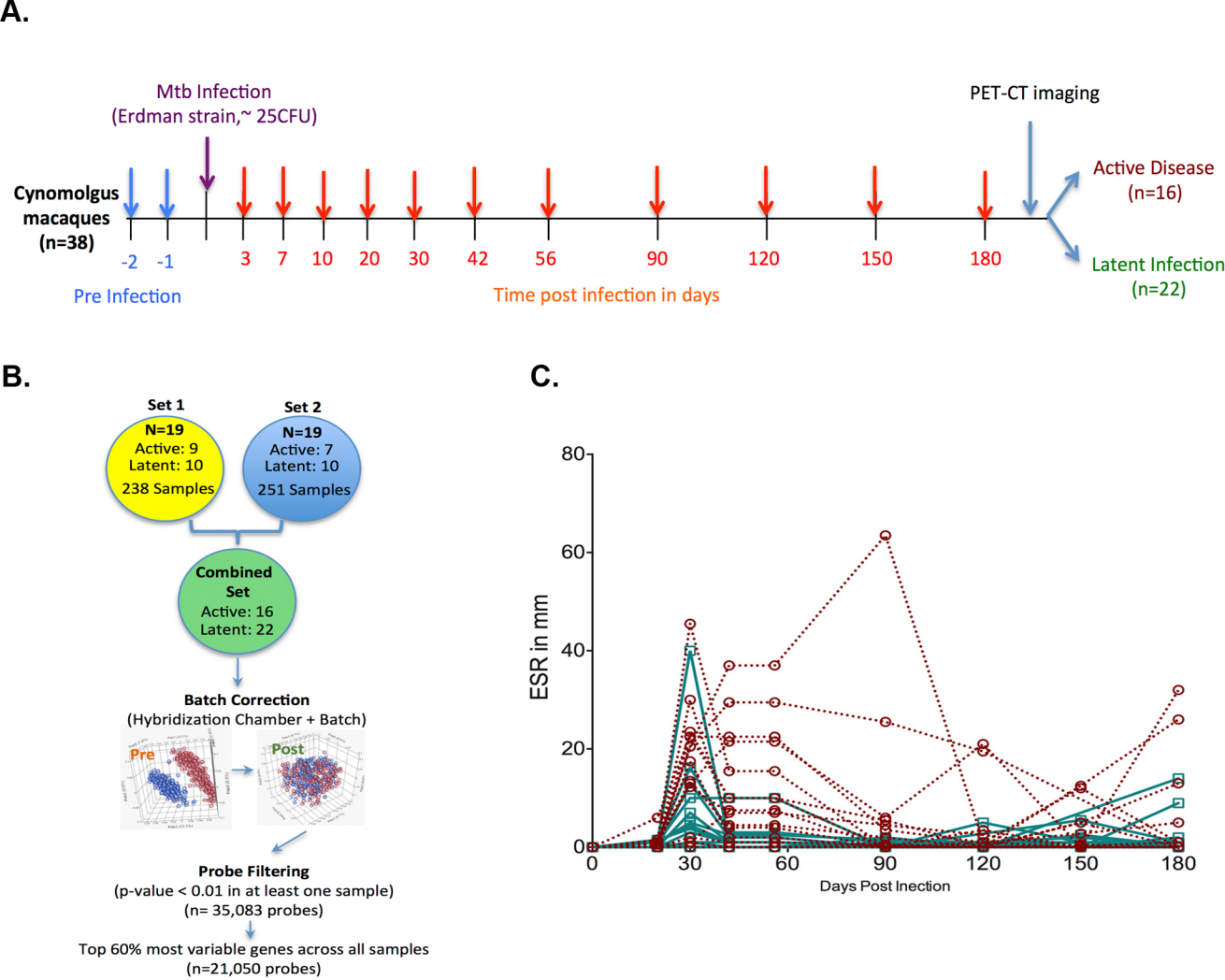

Figure S1: Study Design. **(A)** Schematic representation of the study design with sampling and infection time points. Whole blood for RNA-expression profiling (n=38) and cellular composition (n=19) was collected. NHPs were diagnosed to have active disease at the time of clinical presentation of disease (90-180 days post infection) or declared to have latent infection (180 days post infection). Radiological imaging (PET/CT) was performed after clinical outcome was declared. **(B)** Samples were collected and processed in two independent sets. RNA-expression profiles were batch corrected in the final combined dataset and filtered based on expression and overall variability. **(C)** Erythrocyte sedimentation rate (ESR) in millimeters (mm) during Mtb infection. Each line indicates an individual animal. Animals that developed active disease are in maroon dotted line, while those animals that remained with latent infection are in green solid lines.

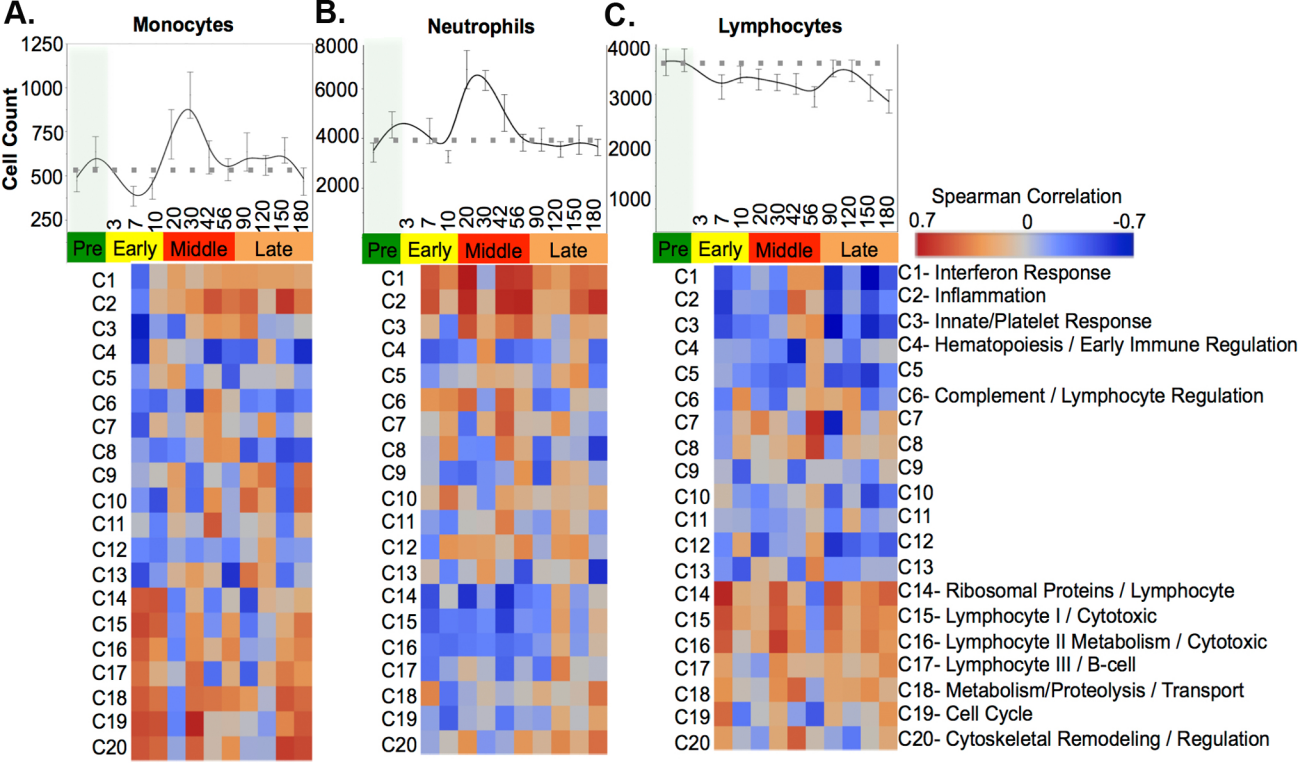

Figure S2: Cross-correlation of gene signatures and circulating cell populations reveal transient changes in transcriptional programming following Mtb infection. Changes in circulating monocyte **(A),** neutrophil **(B)** and lymphocyte **(C)** populations accompany correlation changes with k-means 20 transcript clusters. Error bars represent SEM at each time point for all 19 macaques. Below each cell count plot is a correlation matrix for each cell type with each K=20 transcript cluster from day 7 p.i to day 180 p.i. The heat map scale shows the strength of spearman's correlation ranging from 0.7 (highest positive correlation) to -0.7 (highest negative correlation).

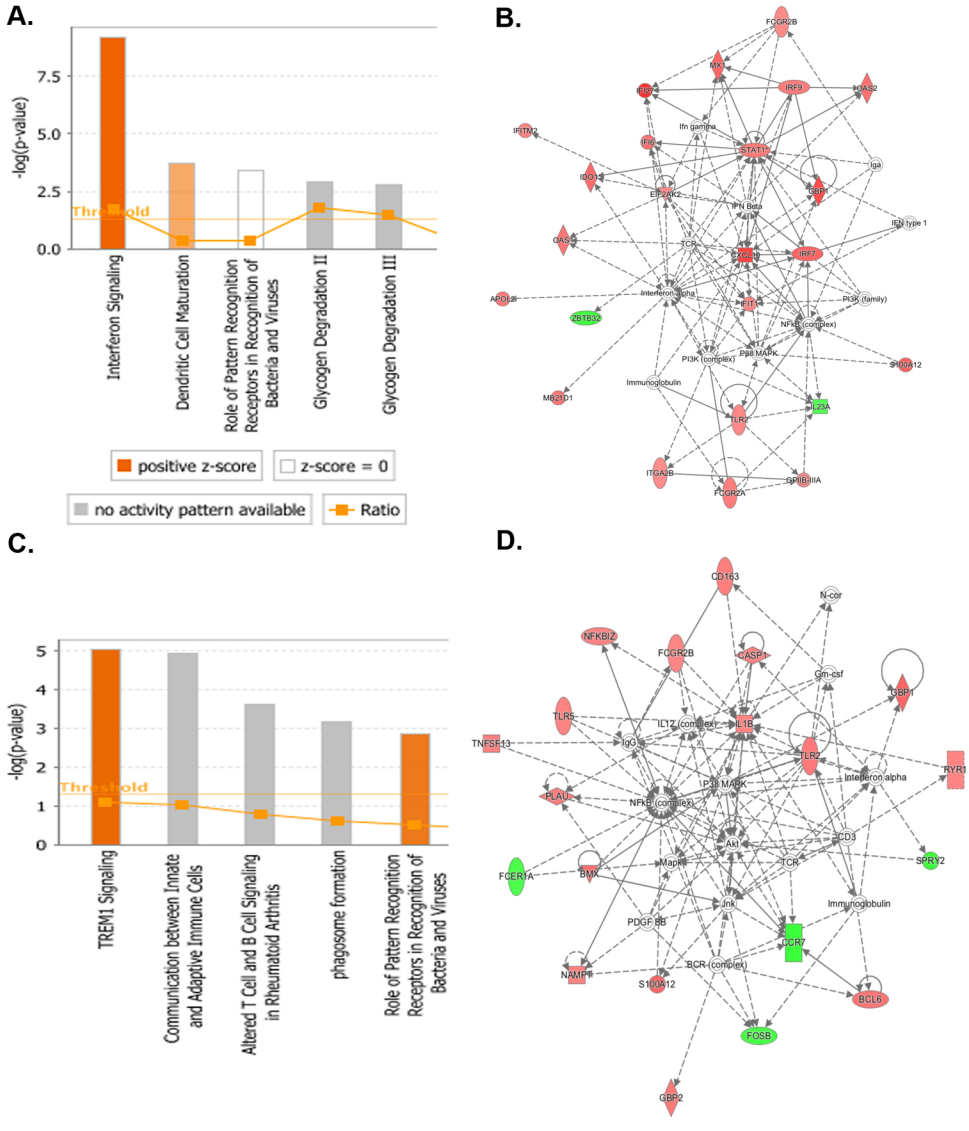

Figure S3: Pathway and network analysis: IPA canonical pathway analysis was performed for 109 transcripts that are differentially expressed by fold change >1.5 and p<0.05 (Mann-Whitney unpaired T and Benjamin-Hochberg for MTC) between active disease and latent infection. **(A)** Top 5 canonical pathways (between high and low FDG lung avidity) with highest representation, which includes Interferon signaling and dendritic cell maturation. **(B)** The top networks associated with the transcripts are shown (red are up regulated and green are down regulated). Similarly, IPA canonical pathway analysis was performed for 91 transcripts that are differentially expressed by fold change >1.5 and p<0.05 (Mann-Whitney unpaired T test with Benjamin-Hochberg for MTC) between animals with high or low lung FDG avidity. **(C)** The top 5 canonical pathways (between active and latent outcomes) with greatest differential expression. The most dominant pathway associated with this signature is TREM1 signaling, followed by interaction of innate and adaptive immune response, altered T and B cell function, and phagosome formation. **(D)** The top networks associated with the transcripts between active and latent outcomes are shown. Highlighted in red are up regulated and green are down regulated transcripts.

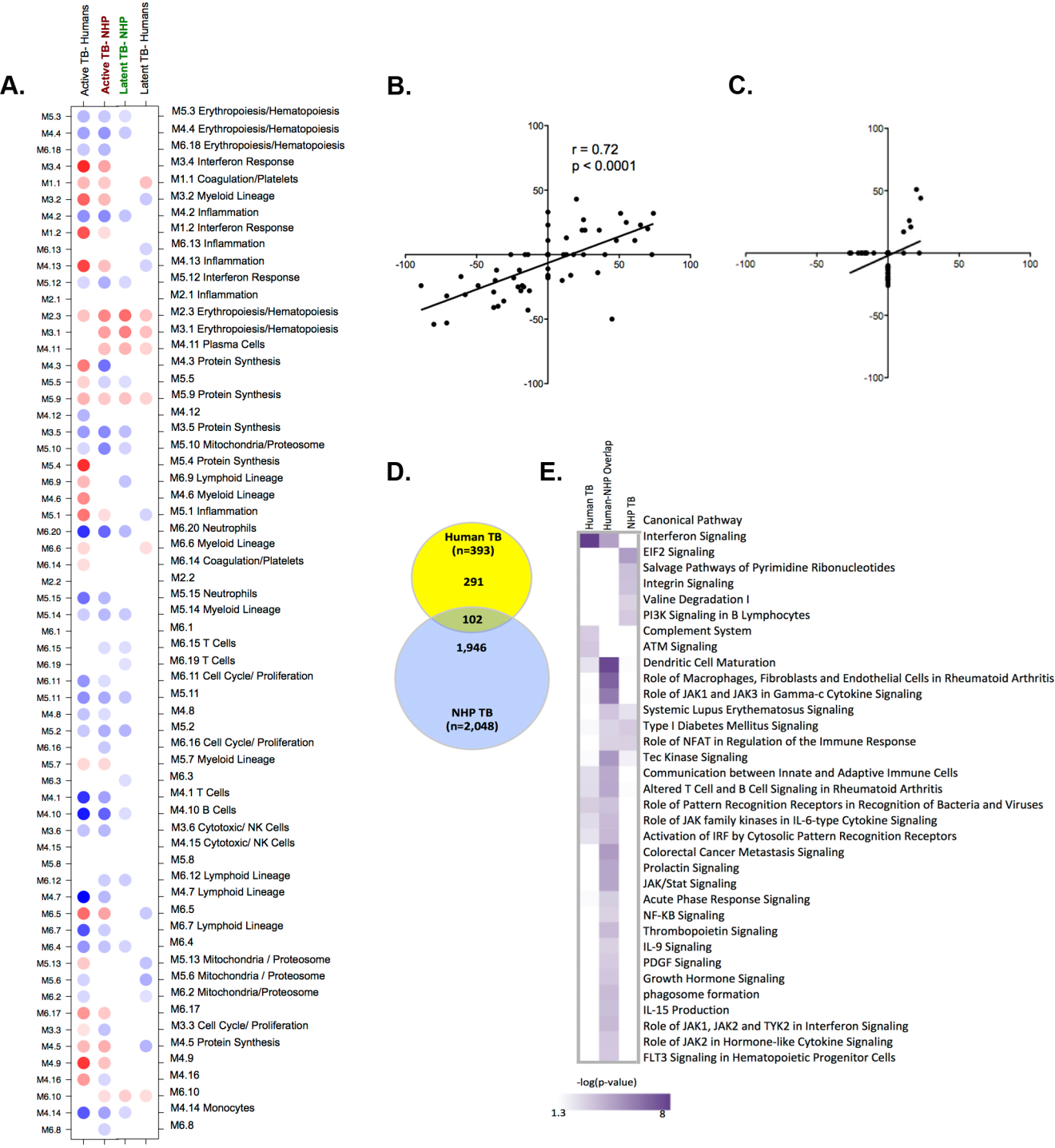

Figure S4: **Human and NHP active disease signatures are concordant.** To evaluate the similarities between human and NHP TB signatures at the time of diagnosis, we compared data from Berry, et al. 2010, a human TB study that utilized the same microarray platform and processing methodologies as our study. **(A)** Human and NHP active and latent infection signature are plotted together. Red color represents over expression over pre-infection (NHP) or healthy controls (Human), whereas blue color represent under expression relative to these baselines. The intensity of the color represents the degree of differential expression from baseline. In **(B)**, we performed a non-parametric spearman's correlation of the signatures between active TB in humans and NHP. We observed that these signatures have a significant positive correlation (spearman's r=0.72, p<0.0001), indicating concordance between active TB signatures in NHP and humans. **(C)** Spearman correlation between latent infection in human and NHP. **(D)** Overlap between the active TB signature identified in Berry *et. al.*, (n=393) and the differentially expressed active signature identified at the time of clinical diagnosis. **(E)** Metacore IPA analysis of gene lists both unique and shared between the human (n=393) and macaque (n=2,048) active signatures (p<0.05).

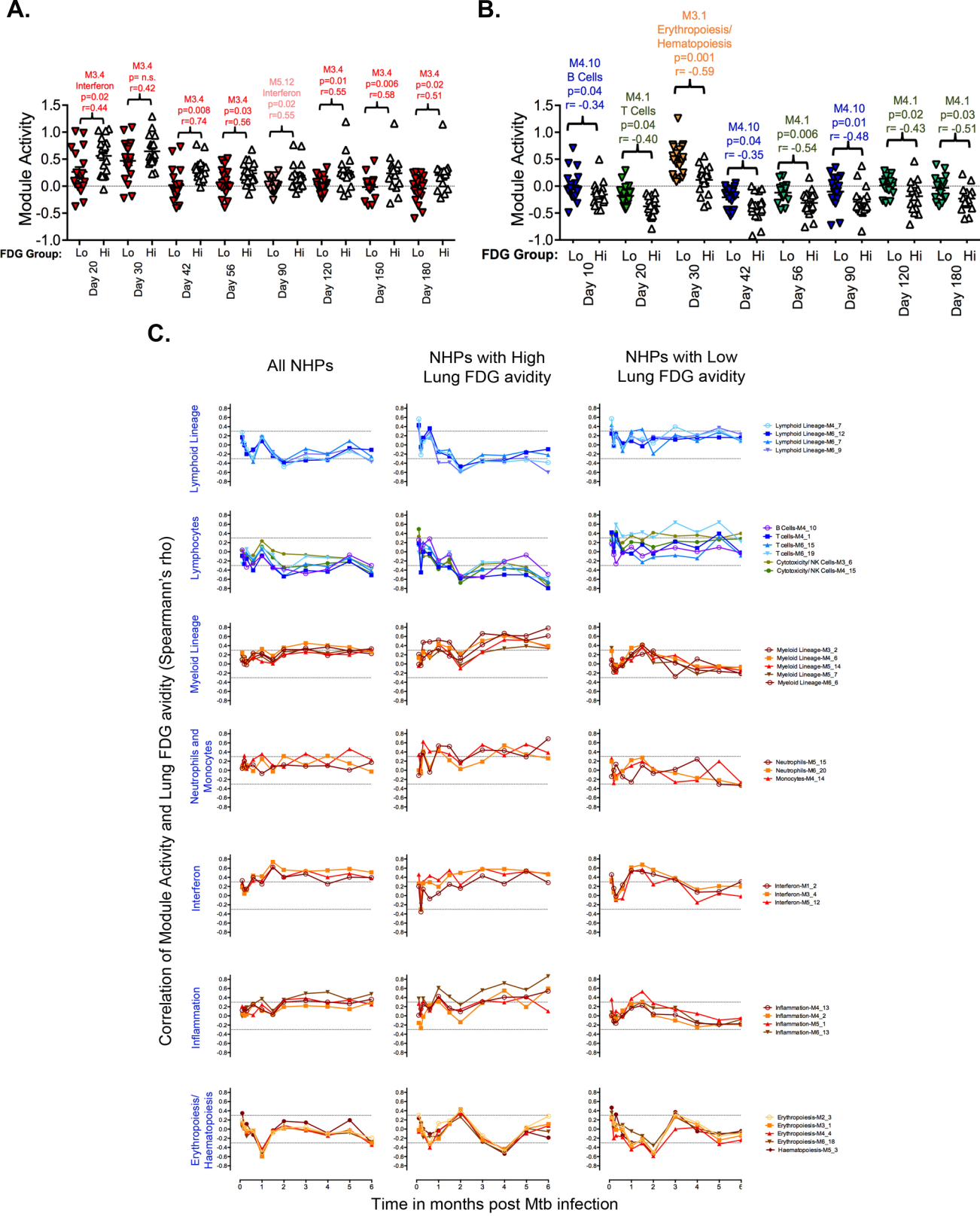

Figure S5: Differential activity of lung FDG avidity correlated with module activity after Mtb infection. **(A)** Modules with the greatest positive spearman-correlation (r) values with disease severity, measured by lung FDG avidity, at each time point post Mtb-infection are presented. At each time point module activity scores was compared between low (lo, colored inverted triangles) and high (hi, open triangles) lung FDG avidity groups using a nonparametric Mann-Whitney test (p-value). **(B)** The module with the greatest negative spearman-correlation (r) with disease severity, measured by lung FDG avidity, at each time point post-infection are presented. At each time point module activity scores are shown for both low (shaded triangles) and high (open triangles) FDG groups were compared using a nonparametric Mann-Whitney test (p-value). **(C)** Module activity and lung FDG avidity was correlated in (i) all animals, (ii) animals with high FDG and (iii) animals with low FDG. Spearman correlation rho values were plotted for modules over time in months post Mtb infection. Modules are grouped based on the function or cell type. Cooler color (blue, green) indicates modules that are under expressed and warm color (yellow, red, brown) indicates modules that are over expressed from baseline. A correlation value below or above the dotted line indicates significant negative or positive correlation between lung FDG avidity and module activity, respectively.